This article was downloaded by: [Canadian Research Knowledge Network]

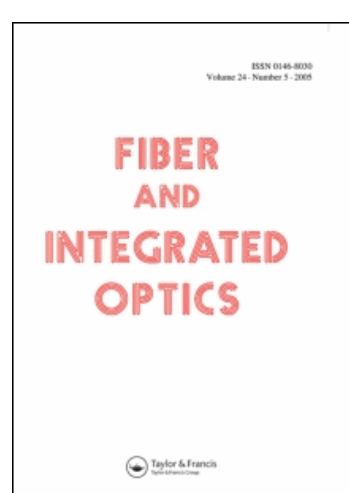
On: 13 April 2011

Access details: *Access Details:* [subscription number 932223628]

Publisher Taylor & Francis

Informa Ltd Registered in England and Wales Registered Number: 1072954 Registered office: Mortimer House, 37-

41 Mortimer Street, London W1T 3JH, UK



#### Fiber and Integrated Optics

Publication details, including instructions for authors and subscription information: http://www.informaworld.com/smpp/title~content=t713771194

#### Q-Factor Microcavity Design Based on 12-Fold Photonic Quasicrystals

Ali Rostami<sup>ab</sup>; Samiye Matloub<sup>a</sup>; Ali Haddadpour<sup>a</sup>

<sup>a</sup> Photonics and Nanocrystal Research Lab (PNRL), Faculty of Electrical and Computer Engineering, University of Tabriz, Tabriz, Iran <sup>b</sup> School of Engineering-Emerging Technologies, University of Tabriz, Tabriz, Iran

Online publication date: 31 March 2011

To cite this Article Rostami, Ali , Matloub, Samiye and Haddadpour, Ali(2011) 'Q-Factor Microcavity Design Based on 12-Fold Photonic Quasicrystals', Fiber and Integrated Optics, 30: 2, 125 - 138

To link to this Article: DOI: 10.1080/01468030.2011.557141 URL: http://dx.doi.org/10.1080/01468030.2011.557141

#### PLEASE SCROLL DOWN FOR ARTICLE

Full terms and conditions of use: http://www.informaworld.com/terms-and-conditions-of-access.pdf

This article may be used for research, teaching and private study purposes. Any substantial or systematic reproduction, re-distribution, re-selling, loan or sub-licensing, systematic supply or distribution in any form to anyone is expressly forbidden.

The publisher does not give any warranty express or implied or make any representation that the contents will be complete or accurate or up to date. The accuracy of any instructions, formulae and drug doses should be independently verified with primary sources. The publisher shall not be liable for any loss, actions, claims, proceedings, demand or costs or damages whatsoever or howsoever caused arising directly or indirectly in connection with or arising out of the use of this material.

Fiber and Integrated Optics, 30:125–138, 2011 Copyright © Taylor & Francis Group, LLC ISSN: 0146-8030 print/1096-4681 online DOI: 10.1080/01468030.2011.557141



# Q-Factor Microcavity Design Based on 12-Fold Photonic Quasicrystals

## ALI ROSTAMI,<sup>1,2</sup> SAMIYE MATLOUB,<sup>1</sup> and ALI HADDADPOUR<sup>1</sup>

<sup>1</sup>Photonics and Nanocrystal Research Lab (PNRL), Faculty of Electrical and Computer Engineering, University of Tabriz, Tabriz, Iran

**Abstract** A microcavity based on 12-fold photonic quasicrystals is achieved by the aid of alteration in the proposed structure. The central air hole is missed, and the three nearest surrounding holes radiuses and positions are modified in order to optimize the Q-factor. In addition, special fine variations are imposed on the mentioned parameters to shift the resonant wavelength in the 1.55- and 1.31- $\mu$ m window bands. One of the predominant features of this microcavity structure is its capability of obtaining a Q-factor of about  $2 \times 10^6$  in the 1.55- $\mu$ m wavelength window band, which is the most desirable wavelength in the optical telecommunication.

**Keywords** high-quality factor, microcavity, photonic quasicrystal

#### 1. Introduction

During the past decade, following up on some recent discoveries in solid-state physics [1, 2] and based on the theory of "aperiodic tilings" [3], resulted in a new class of ordered structures called "photonic quasicrystals" (PQCs), which corroborate the possibility of obtaining analogous properties as exhibited by photonic crystals (PCs), with significant potential improvements achievable via a judicious exploitation of the additional degrees of freedom inherently available in aperiodic geometries [4–6].

PQCs are artificial dielectrics in homogenous media, where scattering centers are located in the vertices of the quasiperiodic tiling of space. These aperiodically ordered structures have neither true periodicity nor translational symmetry but have a quasiperiodicity that exhibits long-range translational and orientional order [7]. PQCs possess numerous appealing properties, such as complete a photonic bandgap [8, 9], superprism [10], and negative refraction index [11]. These properties could lead to novel applications, such as optical filters [12], PQC fibers [13], lasers, and microcavities [14, 15].

Dielectric microcavities have attracted much attention due to their ability to entrap photons in the visible and near infrared (NIR) regions of the electromagnetic spectrum

Received 20 July 2010; accepted 19 January 2011.

Address correspondence to Dr. Ali Rostami, Photonics and Nanocrystal Research Lab (PNRL), Faculty of Electrical and Computer Engineering, School of Engineering–Emerging Technologies, University of Tabriz, Tabriz, 51666, Iran. E-mail: rostami@tabrizu.ac.ir

<sup>&</sup>lt;sup>2</sup>School of Engineering–Emerging Technologies, University of Tabriz, Tabriz, Iran

via total internal reflection [16]. Such photon confinement can be used for various purposes, ranging from fundamental studies on quantum electro-dynamics [17] to more applied fields, such as the development of microscopic laser sources, tunable filters, and transducer mechanisms for optical sensing [18].

In order to characterize the microcavity, the field distribution in the Fourier space and time domain to estimate the spectrum and quality factor (Q-factor) is studied. The cavity Q-factor is determined from the spectral width ( $\Delta\lambda$ ) of the transmission spectrum ( $Q \approx \lambda/\Delta\lambda$  for the cavity mode resonance at  $\lambda$ ). While this is valid for a low Q-factor cavity, in general, the cavity Q-factor may be obtained by estimating the cavity photon life time ( $\tau$ ) from  $Q = \omega_0 \tau$ , where  $\omega_0$  is the resonant cavity mode frequency [16].

Microcavities based on PC structures can be realized by the aid of particular methods exerted on the structure comprised of various approaches, such as missing central or several holes in the primitive structure. For an instance, the cavity structure, in which the initial structure is a hexagonal PC, was designed by missing 7 holes and shifting the positions of the 12 nearest holes, moving 6 of them inward and 6 of them outward [19]. One of the most significant features of these microcavities is their ability of strong mode confinement. In other words, gaining access to a large amount of *Q*-factor in these structures is one of the most outstanding concerns to which considerable recent attention has been paid by several research groups.

In this direction, several methods have been exploited in order to optimize the Q-factor. An ultra-high Q-factor of larger than one million has been reported based on the PC double hetrostructure [20], and in the 1D arrangement of a PC, the seven-hole taper yields the maximum Q-factor of about  $1.4 \times 10^6$  in the waveguide microcavity [21]. Another example would be in the waveguide-section microcavities, the cavity structure is created by three missing holes, called (L3). The mentioned structure's Q-factor can reach as high as approximately  $10^5$  [22]. Another technique has been proposed in the hexagonal PC by missing the central hole and modifying the positions of cavity side holes [23]; meanwhile, in another microcavity structure based on a PC with a hexagonal array, a Q-factor of 7,700 at 1,535 nm was obtained [19]. Finally, in the recently reported works that are pertinent to the cavity based on PC structures, by using optimized irregular structures for PC cavities, one can greatly reduce the material requirement and device size, as mentioned by Bauer et al. [24]. Utilizing a 2D truncated PC cavity with an optimal Q-factor and moving the rods from the lattice positions, an increment in the Q-factor value by orders of magnitude, e.g., from 130 to 11,000, was achieved [24].

Following up on the discovery of quasicrystals in solid-state physics, similar procedures in the direction of boosting the Q-factor have been realized. For instance, the 12-fold PQC structure was used as a microgear laser by missing the seven nearest holes [14, 15]. Another elaborative study on mode confinement in PQC point-defect cavities has been realized by missing the central rod of a 12-fold PQC [25]. All in all, numerous microcavity design methods and approaches have been employed and investigated in these studies, and in many cases, the experimental achievement of a high Q-factor is predicated on the ability to fabricate the design with a small margin for error.

In this work, the microcavity based on a 12-fold PQC is studied. The process of microcavity realization constitutes two steps: missing the central air hole and modification in the neighboring side holes sizes and positions. By means of this, a high Q-factor of order  $10^7$  is achieved. Considering the fact that a resonant wavelength peak should be in the range of optical communication, some other alteration have been exerted on the proposed microcavity structure. Consequently, an optimum structure with a remarkable Q-factor value has been obtained. The other spectacular characteristics of this microcavity

is its aptitude of enhancing a Q-factor to the amount of about  $2 \times 10^6$  in the 1.55- $\mu$ m wavelength window band, which is the most desirable wavelength in the optical communication. It is good to mention that the attained Q-factor has not been reported in this wavelength up to now.

The organization of this article is as follows. In Section 2, the microcavity based on a 12-fold PQC is proposed. In Section 3, the microcavity optimized structure is described, and also the simulation results are presented. In Section 4, the *Q*-factor dependence on other parameters of the structure is investigated. Finally, the article ends with a conclusion.

#### 2. Microcavity Based on 12-Fold PQCs

The basic structure that will be investigated here is Stampfli dodecagon that is shown in Figure 1b. Figure 1 was constructed by following the random-Stampfli inflation rules [8, 26, 27], which show self-similarity properties. This means that by starting from a structure characterized by some symmetry; they will be maintained by an enlarged similar structure. Figure 2 shows the process of forming a Stampfli quasicrystal. Two basic cells, a square, and a triangle are arranged to realize the 12-fold symmetry. Starting from the center of the figure and moving to the outer regions, its 19 points have the coordinates (0,0),  $[(\pm\sqrt{3}/2,\pm1/2),(0,\pm1)]$ , and  $[(\pm(1+\sqrt{3}/2),\pm1/2),(\pm1/2,\pm(1+\sqrt{3}/2)),(\pm(1/2+\sqrt{3}/2),\pm(1/2+\sqrt{3}/2))]$ . Next, by zooming out of  $2+\sqrt{3}$  (the equivalent of the golden ratio for Penrose tilings) and substituting each point of Figure 2b with the cell of Figure 2a, a larger quasicrystal is obtained, as shown in Figure 1. In the end, by repeating the previous steps, the structure can be enlarged indefinitely.

A cavity geometry based on the Stampfli 12-fold PQC is proposed. Introducing a microcavity into a PQC structure can be achieved in two ways: by missing one or more air

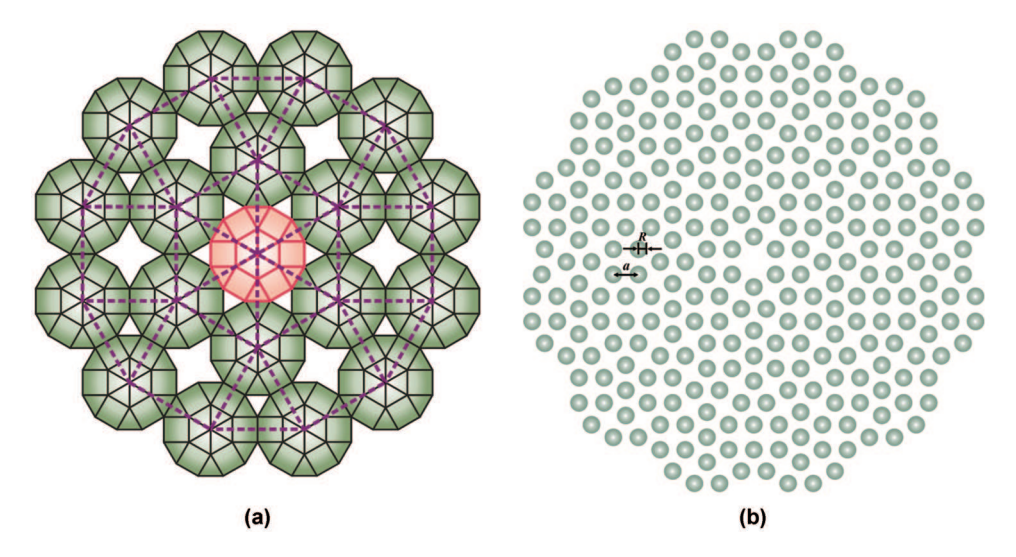


**Figure 1.** (a) Nineteen dodecagonal cores have been put together to enlarge the 12-fold Stampfli quasicrystal. (b) The simplest cavity structure of a 12-fold PQC that has been accomplished by missing the central hole. The cavity is composed of 289 air holes with a radius set to be R = 0.42a, where a is the lattice constant of the structure (a = 390 nm), and the refractive index of the background is 3.4 ( $n_{background} = 3.4$ ), which corresponds to GaAs at 1.55  $\mu$ m.

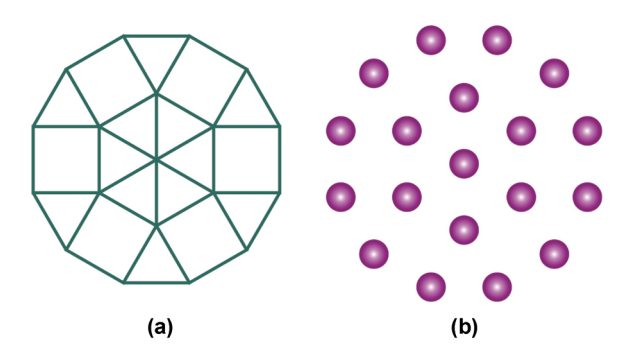


**Figure 2.** (a) The two basic constituent parts, square and equilateral triangle, of a 12-fold Stampfli quasicrystal forming the core of the structure and (b) only the vertices of squares and triangles are highlighted.

holes, known as a donor-type microcavity [22, 28, 29], or by enlarging an air hole, known as an accepter microcavity [28, 29], in which a donor-type microcavity has been utilized in the proposed structure. The simplest cavity structure of a PQC that has been created by missing the central air hole is shown in Figure 1b. The illustrated structure is the initial cavity geometry. The PQC pattern consists of 289 air holes with radius set to R = 0.42a, where a is the lattice constant of the structure (a = 390 nm). The refractive index of background is 3.4 ( $n_{background} = 3.4$ ), which corresponds to GaAs at  $1.55 \mu m$ .

The microcavity has been analyzed using the finite-difference time-domain (FDTD) simulation technique with perfectly matched layer (PML) boundary conditions at the boundary of the simulation region. Simulations were repeated with different space and time resolution to verify their stability and reproducibility [30, 31]. With the aid of this technique, the Q-factor was calculated for the mentioned structure, which is equal to  $3.27 \times 10^5$  at the  $1.23-\mu m$  resonant wavelength. It can be deduced that this structure has the aptitude of boosting the Q-factor amount to a larger value in comparison with the microcavity based on a PC. Augmenting the Q-factor, accompanied by shifting the resonant wavelength to the desired optical telecommunication wavelength, will be discussed in detail in the subsequent section.

The mentioned microcavity characteristics have been modified within numerous variations in the parameters of the structure. The design process consists of engineering three elements: (1) the radius of neighboring air holes, (2) the positions of closer air holes from the center, and (3) the refractive index of background material. To accomplish an optimal microcavity structure that realizes the mentioned features, six nearest-neighbor holes, the second and third rotational row radiuses around the defect cavity ( $R_1$ ,  $R_2$ , and  $R_3$ , respectively) are nominated, which is illustrated in Figure 3a. Also, the radial distance of the three nearest rows surrounding the microcavity is indicated as  $D_1$ ,  $D_2$ , and  $D_3$ , respectively.

As is known, the  $k_{\parallel}$  components (in-plane wave vector) of the cavity mode that lie inside the leaky region must be reduced in order to achieve a high Q-factor value [32]. Basically, symmetries are applied to enforce special boundary conditions on the momentum space representation of the mode, so that the in-plane electric field polarizations at  $k_z=0$  (out-of-plane wave vector) are eliminated. To further reduce the in-plane momentum components inside the leaky region, the geometries of the lattice structure surrounding the defect are modified. This, in essence, changes the Bragg reflection conditions at the

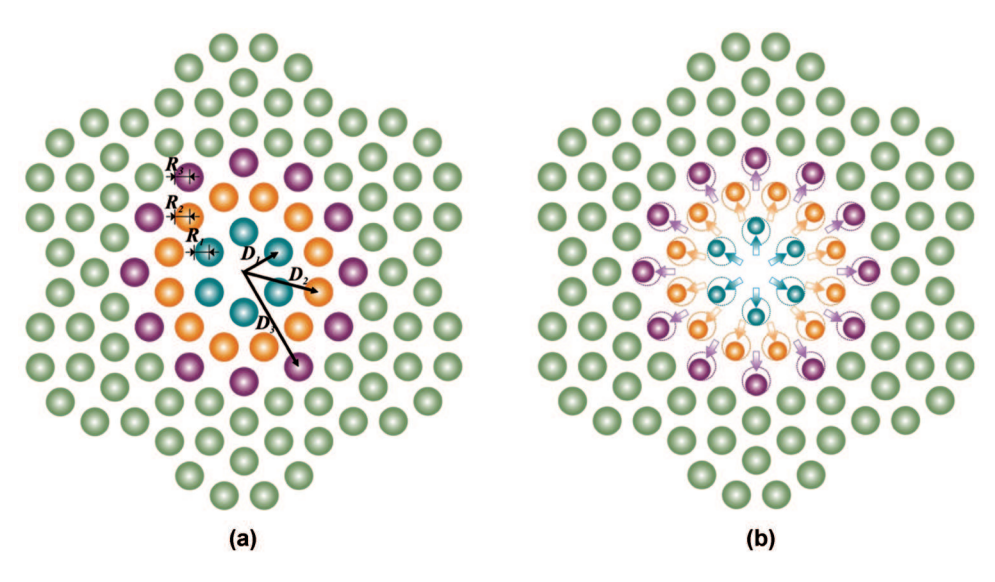


**Figure 3.** (a) Defining six nearest-neighbor holes, second and third rotational row radiuses around the defect cavity, as  $R_1$ ,  $R_2$ , and  $R_3$ , respectively, and the radial distance of three nearest row surrounded microcavities as  $D_1$ ,  $D_2$ , and  $D_3$ , respectively. (b) Modified microcavity structure. The three nearest rows around the defect cavity are reduced in size and pushed away from the center simultaneously.

cavity edges. Doing so allows the light to penetrate deeper inside the surrounding lattice and reflect gently and perfectly [33].

According to the various techniques mentioned in the introduction, fine variations in the three nearest row positions around the central hole and missing the central hole itself have been exploited to augment the Q-factor. In this direction, the three nearest rows around the defect cavity are reduced in size and pushed away from the center simultaneously, as in Figure 3b. The corresponding results of employing the mentioned modification are in Table 1. It can be inferred from the results in Table 1 that the amount of Q-factor is increased extraordinarily, and the corresponding resonant wavelength can be tuned in a range of desired wavelengths from the optical communication point of view. The subsequent section investigates enlarging the Q-factor in the 1.55- $\mu$ m and 1.31- $\mu$ m window bands in more detail.

 Table 1

 Optimized simulation results of two and three nearest row modification

	Radius (nm)	Distance (nm)	Q-factor	λ (nm)
R = 165  nm	$R_1 = 0.28a$	$D_1 = 1.15a$	$1.6520 \times 10^7$	1,356
$n_{background} = 3.39$	$R_2 = 0.36a$ $R_1 = 0.26a$	$D_2 = 2.00a$ $D_1 = 1.16a$	$1.5619 \times 10^7$	1,403
	$R_2 = 0.35a$ $R_3 = 0.32a$	$D_2 = 2.00a$ $D_3 = 2.73a$		

#### 3. Improvement of Q-Factor

As mentioned earlier, exploiting the delicate variations in the positions of the three nearest rows, and simultaneously reducing their sizes, can be a salient approach to enhance the Q-factor amount by also considering the optical communication range of wavelength. The very high Q-factor values achieved in [34] are not necessarily useful in practical situations, such as dense wavelength-division-multiplexing (DWDM) telecommunications, where the channel separation (e.g., 50 GHz) is typically much larger than the full-width at half-maximum (FWHM) of approximately 200 MHz that corresponds to a Q-factor of one million. Here, the enlargement was done for the Q-factor amount in the 1.55- $\mu$ m and 1.31- $\mu$ m window bands. The size and positions of the three nearest neighboring holes are modified to reduce the in-plane radiation losses to increase the Q-factor. By fine tuning the structural parameters, sizes, and positions, the optimum values are shown in Table 2, where the Q-factor has been boosted in the desired wavelength interval. The Q-factor of about  $2 \times 10^6$  in the 1.55- $\mu$ m wavelength window band, which is the most desirable target in this section, can be achieved. So far, this amount of Q-factor has not been reported in this wavelength.

For extracting the properties of PQC devices, some numerical methods must be employed to study and analyze them. The plane wave expansion (PWE) and multiple scattering theories are interesting methods on the frequency domain for these structures [35]. The speed of computing in the above-mentioned methods is high, which is the preference, but the problem was only the confinement in calculating the stationary state. Another effective method for the analysis of PQC structures is FDTD, which is currently a popular numerical solution method [35]. FDTD is a powerful method for solving Maxwell's equations in the time domain due to its simplicity. Resonant frequencies and the Q-factor are calculated using the FDTD method. The grid size is 0.05a in the x, y direction. By applying PML boundary conditions as absorbing boundaries and using a much smaller number of time steps, an accurate Q-factor value has been achieved. There are some reasons that play an important role, obliging the sophisticated calculation of the Q-factor for high Q-factor cavities:

- separating the decay of the envelope from the underlying sinusoidal signal is difficult since the fields are typically real valued;
- if there are multiple resonant modes, they will interfere with each other in the time domain, making it hard to estimate the decay rate.

Table 2 Optimum *Q*-factor values for 1.55- $\mu$ m and 1.31- $\mu$ m window band

	Radius (nm)	Distance (nm)	Q-factor	λ (nm)
$R = 145 \text{ nm}$ $n_{background} = 3.39$	$R_1 = 0.3a$ $R_2 = 0.3a$ $R_3 = 0.3a$	$D_1 = 1.07a$ $D_2 = 2.00a$ $D_3 = 2.80a$	$2.08 \times 10^{6}$	1,549.4
$R = 165 \text{ nm}$ $n_{background} = 3.39$	$R_1 = 0.17a$ $R_2 = 0.27a$ $R_3 = 0.32a$	$D_1 = 1.25a$ $D_2 = 2.09a$ $D_3 = 2.73a$	$2.33 \times 10^{6}$	1,311.7

So, the above-mentioned have been resolved problems by

- · accurately calculating the envelope of the time-domain field signal and
- isolating each resonance peak in the frequency domain using a Gaussian filter, and then taking the inverse Fourier transform to calculate the time decay separately for each peak; the slope of the time decay is then used to calculate the Q factor.

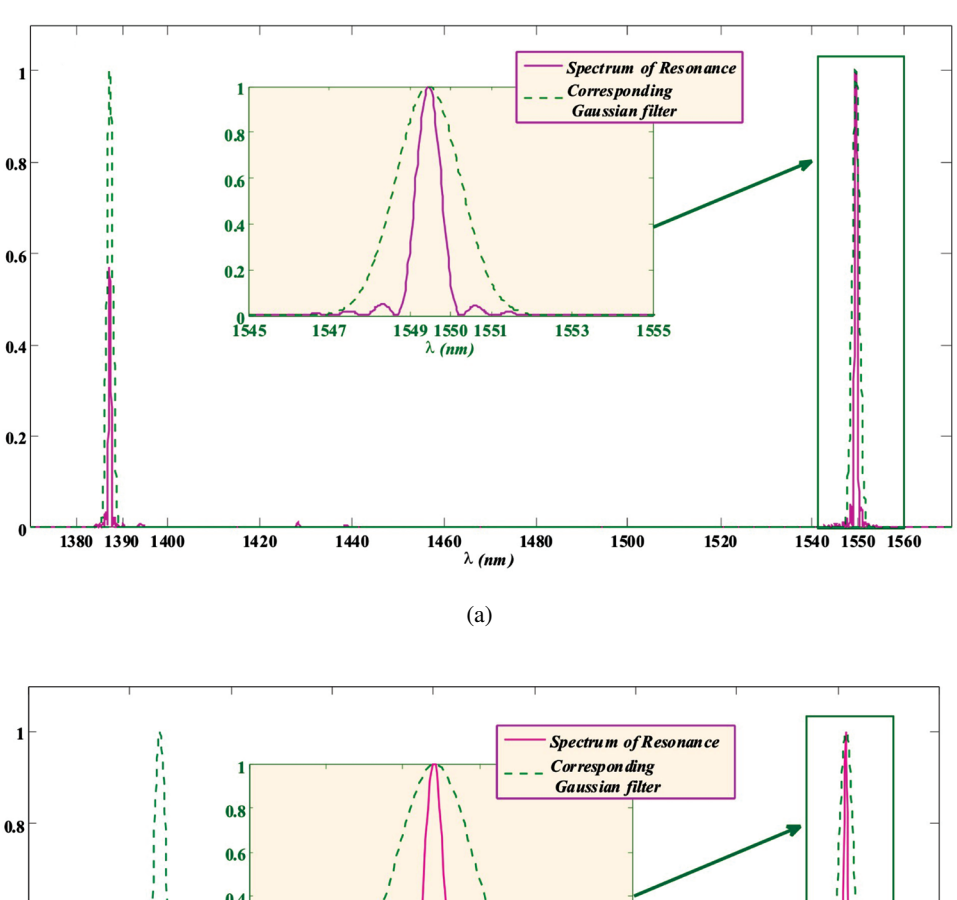
By means of this technique, the resonance peak in the frequency domain and corresponding Gaussian filter are illustrated for both the 1.55- $\mu$ m and 1.31- $\mu$ m window bands in Figure 4. In addition, the envelope of the time-domain field signal for mentioned wavelength is illustrated in Figure 5. The final step in the microcavity analysis is to look at the mode profiles of the proposed structure. The corresponding field distribution for each resonance peaks in the 1.55- $\mu$ m and 1.31- $\mu$ m wavelength window bands are shown in Figures 6a and 6b, respectively. For example, Figure 6a represents the electric field distribution for resonance peak of 1.55  $\mu$ m, and Figure 6b corresponds to a lower wavelength resonance peak ( $\lambda \approx 1.39 \ \mu$ m). In addition, the dependence of the Q-factor on the radius and the refractive index of the dielectric material has been studied and is discussed in the following section.

### 4. Dependence of *Q*-Factor on Background Refractive Index and Radius Variation

Similar studies were also performed in order to understand the influence of radius and background refractive index on the Q-factor value and the corresponding impact on the resonance peak wavelength. Figure 7 shows the maximum value of the Q-factor and wavelength versus refractive index (optimized for each value of refractive index by adjusting the side holes and corresponding distance  $D_i$ ). The Q-factor shows a great tendency to increase, while the refractive index enhances; this ascending trend continues until the maximum Q-factor value is obtained when the refractive index is set to be 3.4. The corresponding impact on the wavelength shifting has been observed, as shown in Figure 7. The resonant peak wavelength also reveals a gradually ascending trend for itself. The optimized structural parameters are included in Table 3, in which the mentioned behavior has been accomplished in the microcavity structure. The importance of Q-factor dependency on the radius of  $R_i$  and corresponding  $D_i$  distances are revealed in

Table 3
Optimized structural parameters for each value of refractive index

	Radius (nm)	Distance (nm)	Q-factor	λ (nm)
$n_{background} = 2.04$ $R = 155 \text{ nm}$	$R_1 = 0.31a$ $R_2 = 0.32a$	$D_1 = 1.09a$ $D_2 = 2.01a$	$2.04 \times 10^{4}$	958.32
$n_{background} = 2.45$ R = 155  nm	$R_1 = 0.34a$ $R_2 = 0.33a$	$D_1 = 1.06a$ $D_2 = 2.00a$	$2.32\times10^5$	1,077.52
$n_{background} = 2.8$	$R_1 = 0.31a$	$D_1 = 1.06a$	$5.57 \times 10^{5}$	1,269.31
$R = 145 \text{ nm}$ $n_{background} = 3.39$	$R_2 = 0.31a$ $R_1 = 0.17a$	$D_2 = 2.00a$ $D_1 = 1.25a$	$2.33\times10^6$	1,311.7
R = 165  nm	$R_2 = 0.27a$ $R_3 = 0.32a$	$D_2 = 2.09a$ $D_3 = 2.73a$		



0.4 0.6 0.2 1306 1308 1312 1314 1316 0.4 0.2 1230 1240 1250 1260 1290 1300 1270 1310 1320 λ (nm) (b)

**Figure 4.** Resonance peak in the frequency domain and corresponding Gaussian filter for (a) 1.55- $\mu$ m and (b) 1.31- $\mu$ m window bands. Needed parameters are included in Table 2.

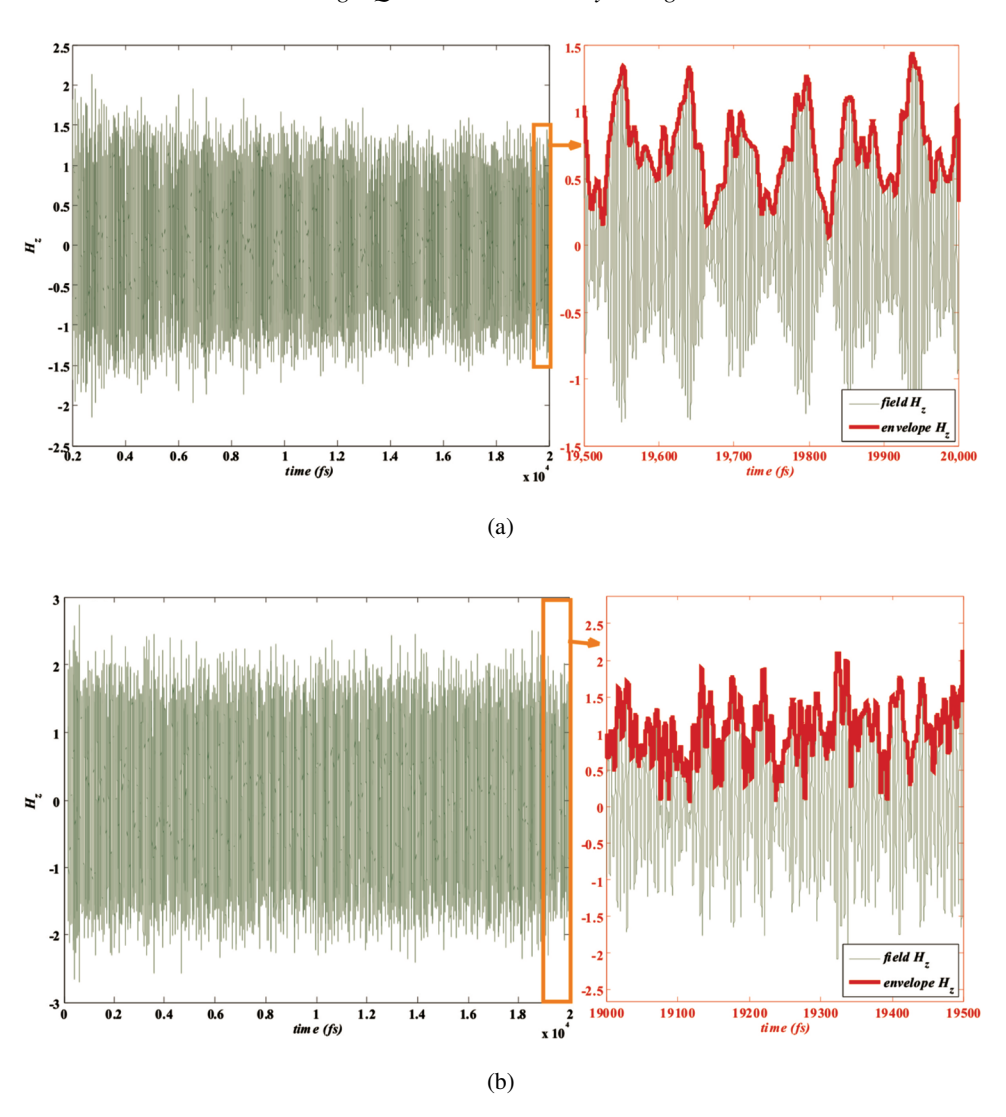


**Figure 5.** The envelope of the time-domain field signal for (a) 1.55- $\mu$ m and (b) 1.31- $\mu$ m window bands. Needed parameters are included in Table 2.

Table 4. This strong reliance can be perceived as a tinge of variation in radius and corresponding distance, resulting in dramatic changes in Q-factor values. The results in Table 4 corroborate this fact.

#### 5. Q-Factor Approaches and Trends

This section explores the overall performances and trends that have been taken by other researchers in accomplishing a microcavity with a high Q-factor more specifically for PC structures, as well as some references pertinent to the PQCs. Their brief approaches are included in Table 5.

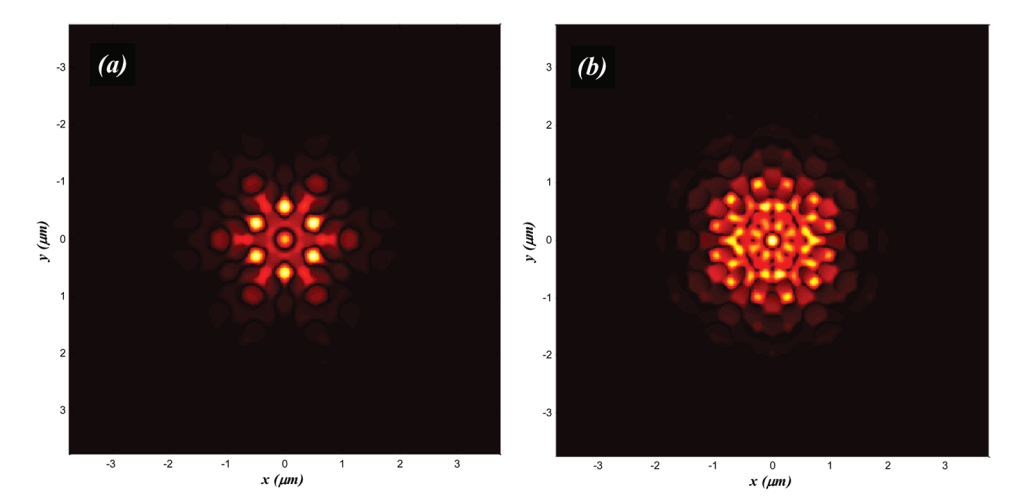


**Figure 6.** The corresponding field distribution for resonance peaks in (a) 1.55- $\mu$ m and (b) 1.31- $\mu$ m wavelength window bands.

As stated before about the proposed structure in more detail, the more significant and predominant feature of this structure is its high Q-factor in the most desirable wavelength window band in an optical communication of 1.55  $\mu$ m; this manifests the aptitude of the PQCs. The Q-factor of about  $2 \times 10^6$  in the 1.55- $\mu$ m wavelength window band can be achieved with the exerted variation expressed in more detail in the previous section. To the best of knowledge of the authors, this amount of Q-factor has not yet been reported in this wavelength.

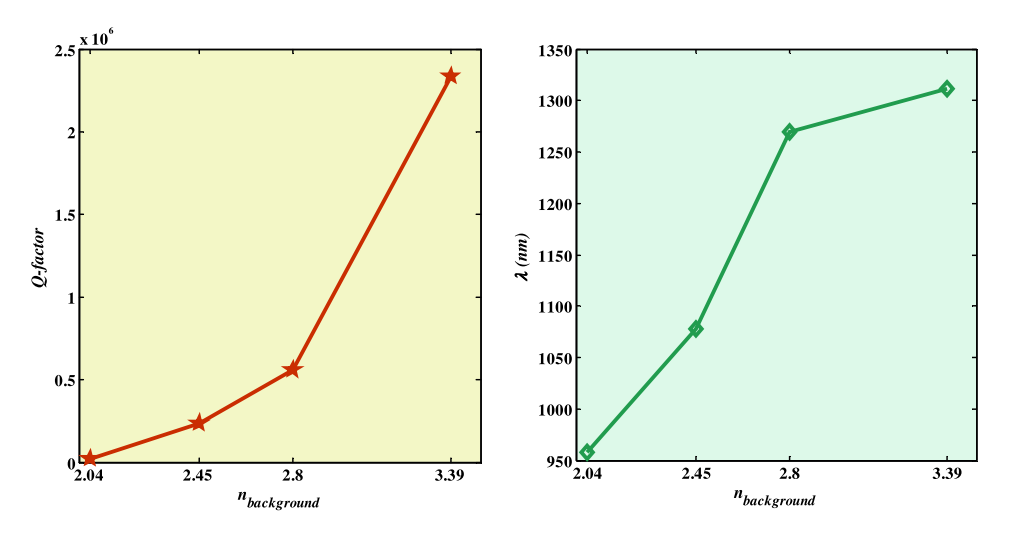


Figure 7. Maximum value of Q-factor versus background refractive index and corresponding wavelength.

Table 4
Structural parameters for each value of size and positions of holes

Radiu	s (nm)	Distanc	ce (nm)		
$R_1$	$R_2$	$D_1$	$D_2$	Q-factor	$\lambda$ (nm)
0.31 <i>a</i>	0.38 <i>a</i>	1.12 <i>a</i>	1.97 <i>a</i>	$6.42 \times 10^{5}$	1,380.5
0.28a	0.36a	1.15a	2.00a	$1.65 \times 10^{7}$	1,355.5
0.26a	0.35a	1.16 <i>a</i>	2.01 <i>a</i>	$7.96 \times 10^{5}$	1,400.5
0.24a	0.34a	1.18 <i>a</i>	2.02a	$9.53 \times 10^{4}$	1,438.0
0.21a	0.31 <i>a</i>	1.21 <i>a</i>	2.04a	$1.74 \times 10^{6}$	1,348.0
0.20a	0.30a	1.23 <i>a</i>	2.06a	$1.45 \times 10^{4}$	1,374.0
0.18a	0.29a	1.24 <i>a</i>	2.07a	$2.10 \times 10^{5}$	1,233.7
0.15a	0.26a	1.27 <i>a</i>	2.09a	$3.54 \times 10^{6}$	1,273.7
0.12a	0.24a	1.31 <i>a</i>	2.12a	$2.61 \times 10^{6}$	1,299.8
0.08 <i>a</i>	0.21 <i>a</i>	1.34 <i>a</i>	2.14 <i>a</i>	$1.55 \times 10^{6}$	1,323.3

**Table 5**Brief approaches for modifying *Q*-factor

Structure	Approaches	Q-factor	
1D PC	Missing and position shifting	$1.4 \times 10^{6}$	
Hexagonal PC	Missing holes	$10^{5}$	
2D PC	Missing and modifying holes	7,700	
2D truncated PC cavity	Moving the rods	11,000	
Proposed 2D 12-fold PQC	Missing and modification in the neighboring side holes sizes and positions	10 <sup>7</sup>	
Proposed 2D 12-fold PQC at 1.55 $\mu$ m	Missing and modification in the neighboring side holes sizes and positions	$2 \times 10^6$	

#### 6. Conclusion

In this work, a microcavity based on a 12-fold PQC was proposed. It was illustrated that the proposed cavity has a high Q-factor to be applied to more applications in integrated optics, optical communications, and especially demultiplexers in DWDM optical systems. In this direction, the most appealing feature of the proposed structure is accessing a high Q-factor value in a 1.55- $\mu$ m window band. The modal analysis of the proposed structure and the Q-factor for different conditions were reported. Finally, the effect of different parameters on the Q-factor of the proposed cavity was investigated.

#### References

- Shechtman, D., Blech, I., Gratias, D., and Cahn, J. W. 1984. Metallic phase with long-range orientational order and no translation symmetry. *Physical Review Letter* 53:1951–1953.
- Levine, D., and Steinhardt, P. J. 1984. Quasicrystals: A new class of ordered structures. *Physical Review Letter* 53:2477–2480.
- Jansssen, T., Chapuis, G., and de Boissieu, M. 2007. Aperiodic Crystals: From Modulated Phases to Quasicrystals. Oxford, UK: Oxford University Press.
- Steurer, W., and Sutter-Widmer, D. 2007. Photonic and phononic quasicrystals. *Journal of Physics D: Applied Physics* 40:229–247.
- Della Villa, A., Galdi, V., Enoch, S., Tayeb, G., and Capolino, F. 2009. Photonic quasicrystals: Basics and examples. In: *Metamaterials Handbook*, vol. I. F. Capolino (Ed.). Boca Raton, FL: CRC Press, chap. 27.
- Chigrin, D. N., and Lavrinenko, A. V. 2009. Photonic applications of two-dimensional quasicrystals. In: *Metamaterials Handbook*, vol. II, F. Capolino (Ed.). Boca Raton, FL: CRC Press, chap. 28.
- 7. Levine, D., and Steinhardt, P. 1986. Quasicrystals I. Definition and structure. *Physical Review B* 34:596–615.
- Zoorob, M. E., Charlton, M. D. B., Parker, G. J., Baumberg, J. J., and Netti, M. C. 2000. Complete photonic band gaps in 12-fold symmetric quasicrystals. *Letters to Nature* 404:740–743.
- Rechtsman, M. C., Jeong, H. C., Chaikin, P. M., Torquato, S., and Steinhardt, P. J. 2008. Optimized structures for photonic quasicrystals. *Physical Review Letter* 101:073902.
- Zhang, X., Li, Z., Cheng, B., and Zhang, D.-Z. 2007. Non-near-field focus and imaging of an unpolarized electromagnetic wave through high-symmetry quasicrystals. *Optics Express* 15:1292–1300.
- Feng, Z., Zhang, X., Wang, Y., Li, Z.-Y., Cheng, B., and Zhang, D.-Z. 2005. Negative refraction and imaging using 12-fold-symmetry quasicrystals. *Physical Review Letter* 94:247402.
- Romero-Vivas, J., Chigrin, D., Lavrinenko, A., and Sotomayor Torres, C. 2005. Resonant add-drop filter based on a photonic quasicrystal. *Optics Express* 13:826–835.
- Kim, S., and Kee, C.-S. 2009. Dispersion properties of dual-core photonic-quasicrystal fiber. Optics Express 17:15885–15890.
- Nozaki, K., and Baba, T. 2004. Quasiperiodic photonic crystal microcavity lasers. Applied Physics Letters 84(24):4875.
- Nozaki, K., Nakagawa, A., Sano, D., and Baba, T. 2003. Ultralow threshold and single-mode lasing in microgear lasers and its fusion with quasi-periodic photonic crystals. *Journal of Selected Topics in Quantum Electronics* 9(5):1330–1332.
- 16. Vahala, K. J. 2003. Optical microcavity. Nature 424:839.
- Gérard, J. M., Sermage, B., Gayral, B., Legrand, B., Costard, E., and Thierry-Mieg, V. 1998. Enhanced spontaneous emission by quantum boxes in a monolithic optical microcavity. *Physical Review Letter* 81:1110–1113.
- Vollmer, F., Braun, D., Libchaber, A., Khoshsima, M., Teraoka, I., and Arnold, S. 2002. Protein detection by optical shift of a resonant microcavity. *Applied Physics Letters* 80:4057.
- Lee, P.-T., Lu, T.-W., Yu, C.-M., and Tseng, C.-C. 2007. Photonic crystal circular-shaped microcavity and its uniform cavity-waveguide coupling property due to presence of whispering gallery mode. *Optics Express* 15:9450–9457.
- Song, B.-S., Asano, T., and Noda, S. 2007. Heterostructures in two-dimensional photoniccrystal slabs and their application to nanocavities. *Journal of Physics D: Applied Physics* 40:2629–2634.
- McCutcheon, M. W., and Loncar, M. 2008. Design of a silicon nitride photonic crystal nanocavity with a quality factor of one million for coupling to a diamond nanocrystal. *Optics Express* 16:19136–19145.

- 22. Akahane, Y., Asano, T., Song, B.-S., and Noda, S. 2003. High-Q photonic nanocavity in a two-dimensional photonic crystal. *Nature* 425:944.
- Ryu, H.-Y., Notomi, M., and Lee, Y.-H. 2003. High-quality-factor and small-mode-volume hexapole modes in photonic-crystal-slab nanocavities. *Applied Physics Letters* 83(21):4294.
- Bauer, C. A., Werner, G. R., and Cary, J. R. 2008. Truncated photonic crystal cavities with optimized mode confinement. *Journal of Applied Physics* 104:053107.
- Di Gennaro, E., Savo, S., Andreone, A., Galdi, V., Castaldi, G., Pierro, V., and Rosaria Masullo, M. 2008. Mode confinement in photonic quasicrystal point-defect cavities for particle accelerators. *Applied Physics Letters* 93:164102.
- Oxborrow, M., and Henley, C. L. 1993. Random square-triangle tilings: A model for twelvefoldsymmetric quasicrystals. *Physical Review B* 48:6966.
- Zhao, H., Zaccaria, R. P., Song, J.-F.., Kawata, S., and Sun, H.-B. 2009. Photonic quasicrystals
  exhibit zero-transmission regions due to translational arrangement of constituent parts. *Physical Review B* 79:115118.
- 28. Akahane, Y., Asano, T., and Song, B. S. 2003. Crystal slabs. Applied Physics Letters 83:1512.
- Noda, S., Hutinan, A., and Imada, M. 2000. Trapping and emission of photons by a single defect in a photonic bandgap structure. *Nature* 407:608.
- Gauthier, R., and Mnaymneh, K. 2005. Photonic band gap properties of 12-fold quasi-crystal determined through FDTD analysis. *Optics Express* 13(6):1985–1998.
- Zito, G., Piccirillo, B., Santamato, E., Marino, A., Tkachenko, V., and Abbate, G. 2009.
   FDTD analysis of photonic quasicrystals with different tiling geometries and fabrication by single-beam computer-generated holography. *Journal of Optics A: Pure and Applied Optics* 11(2):024007.
- Srinivasan, K., and Painter, O. 2003. Fourier space design of high-Q cavities in standard and compressed hexagonal lattice photonic crystals. *Optics Express* 11:579.
- Zhang, Z., and Qiu, M. 2004. Small-volume waveguide-section high Q microcavities in 2D photonic crystal slabs. Optics Express 12:3988–3995.
- 34. Xu, Y., Lee, R. K., and Yariv, A. 2000. Propagation and second-harmonic generation of electromagnetic waves in a coupled-resonator optical waveguide. *Journal of Optical Society of American B* 17:387–400.
- 35. Taflove, A., and Hegnese, S. C. 1998. *Computational Electrodynamics: The Finite-Difference Time-Domain Method*. Boston, MA: Artech House.
- Qiu, M. 2002. Effective index method for heterostructure-slab-waveguide-based two-dimensional photonic crystals. Applied Physics Letters 81:1163–1165).

#### **Biographies**

Ali Rostami received his Ph.D. in photonic/electronic engineering from Amirkabir University of Technology, Tehran, Iran, in 1998. He was on sabbatical leave from the University of Toronto 2004–2005 at the Photonic Group. He is currently a full professor of electronic engineering and photonics science at the University of Tabriz. His teaching and research interests include optical integrated circuits and optoelectronic devices. He is a member of the Optical Society of America. He is the author and coauthor of more than 220 scientific international journals and conference papers and 10 text books in Persian, 4 book chapters, and 2 books. Also, he collaborates with some international journals on their reviewer board and works on the editorial committee of two Iranian journals and one international journal. He has served on several other committees and panels in government and industry and at technical conferences. He is also the founder of the Photonics and Nanocrystals Research Lab (PNRL) at University of Tabriz. The School of Engineering-Emerging Technologies is another project that

he established at University of Tabriz in 2008. Also, he is the chair of the Center of Excellence for Mechatronics since 2005. He was selected as a distinguished researcher of the University of Tabriz several times, and in 2007, he was elected a distinguished researcher in the engineering field in Iran. Since 2008, he has been vice chancellor for research and technology at University of Tabriz.

**Samyle Matloub** is a Ph.D. student at University of Tabriz. Her research area is analysis and design of quasi-periodic structures. She has published more than 25 international journal and conference papers.

**Ali Haddadpour** is an M.Sc. student at University of Tabriz. His research area is related to quasiperiodic structures. He has published one journal and two conference papers.